Synthesis and reactivity of ruthenium(II) complexes containing hemilabile phosphine–thiophene ligands

Olivier Clot,[a] Michael O. Wolf,*[a] Glenn P. A. Yap[b] and Brian O. Patrick[a]

[a] *Department of Chemistry, University of British Columbia, Vancouver, British Columbia, Canada, V6T 1Z1. E-mail: mwolf@chem.ubc.ca*
[b] *Department of Chemistry, University of Ottawa, Ottawa, Canada, K1N 6N5*

The syntheses of two new phosphine–thiophene ligands, 2-(2′-{diphenylphosphino}phenyl)thiophene (dpppth) and 3′-diphenylphosphino-2,2′ : 5′,2″-terthiophene (dppterth) are reported. These ligands react with [RuCl$_2$(PPh$_3$)$_3$] to give [RuCl$_2$(dpppth-*P,S*)$_2$] and [RuCl$_2$(dppterth-*P,S*^{1})$_2$], respectively, which both exist as a mixture of two isomers in solution. [RuCl$_2$(dpppth-*P,S*)$_2$] reacts at 25 °C with carbon monoxide to yield a mixture of [RuCl$_2$(CO)(dpppth-*P*)-(dpppth-*P,S*)] and [RuCl$_2$(CO)$_2$(dpppth-*P*)$_2$], while [RuCl$_2$(dppterth-*P,S*^{1})$_2$] reacts with CO under the same conditions to give only the monocarbonyl complex [RuCl$_2$(CO)(dppterth-*P*)(dppterth-*P,S*^{1})]. Displacement of one of the dppterth ligands in [RuCl$_2$(dppterth-*P,S*^{1})$_2$] with bis(diphenylphosphino)methane (dppm) yields *cis*-[RuCl$_2$(dppm)-(dppterth-*P,S*^{1})] which isomerizes in solution to *trans*-[RuCl$_2$(dppm)(dppterth-*P,S*^{1})]. These complexes react with carbon monoxide to give *trans*-[RuCl$_2$(CO)(dppm)(dppterth-*P*)] and *cis*-[RuCl$_2$(CO)(dppm)(dppterth-*P*)], respectively, in which the thiophene end of the dppterth ligand is displaced by CO. The electronic spectra of these complexes are reported. Crystal structures for [RuCl$_2$(dpppth-*P,S*)$_2$], [RuCl$_2$(CO)(dppterth-*P*)(dppterth-*P,S*^{1})] and *cis*-[RuCl$_2$(dppterth-*P,S*^{1})(dppm)] are reported.

Introduction

Conjugated polymers and oligomers are an interesting and important class of materials which are of use in a wide range of optoelectronic applications, including light-emitting diodes, photovoltaics and field-effect transistors.[1,2] Many approaches are being explored to modify the optical and electronic properties of these materials, amongst them the attachment of metal groups to the conjugated backbone.[3]

We are interested in investigating materials in which metal groups are coupled to oligothiophenes, and have recently examined charge delocalization in compounds in which Fe and Ru centers are inserted into a conjugated backbone.[4–7] A complementary approach involves attaching metal groups *pendant* to the oligothiophene, which permits electronic coupling to the conjugated backbone providing the link between the metal and oligomer is chosen appropriately. A number of research groups have reported materials in which conjugated oligomers or polymers are coordinated to metal centers, and these efforts have been recently reviewed;[3] however, we are particularly interested in creating materials in which the bonding and coordination environment of the metal can be varied while still keeping the complex anchored to the oligomer or polymer. One way in which this may be achieved is *via* a backbone which functions as a hemilabile ligand[8] on a metal to which it is coordinated. The backbone may then be switched between bidentate and monodentate coordination modes, with the electronic coupling between the metal group and the conjugated backbone depending on the coordination mode.

An attractive approach towards this goal is to utilize thiophene, which coordinates weakly to most transition metals, in combination with a strongly coordinating group to generate the hemilabile ligand. Thiophene coordinates *via* several binding modes, from η^1 to η^5,[9–11] and there are several examples known in which thiophene has been incorporated into multidentate thiophene–nitrogen and thiophene–phosphine ligands.[12–24] A number of complexes containing phosphine–thiophene ligands,

such as PPh$_{3-x}$Th$_x$ (Th = 2-thienyl, *x* = 1–3), in which only the phosphine coordinates, have also been reported.[25–33]

We elected to examine bidentate hemilabile ligands incorporating a phosphine and thiophene. This motif was recently employed by Weinberger *et al.* to make polymerizable ruthenium complexes;[12] however, we chose to place the phosphine directly on the oligothiophene backbone to provide the most intimate contact between the metal and the ligand in both mono- and bi-dentate coordination modes. We describe here the syntheses and properties of two new phosphine–thiophene ligands and a series of Ru(II) complexes which incorporate these ligands. In addition, we demonstrate the reactions of carbon monoxide with several of these complexes, resulting in displacement of the thiophene.

Results and discussion

Synthesis of phosphine–thiophene ligands

The phosphine–thiophene ligand dpppth **1** was prepared by reaction of 2-(2′-bromophenyl)thiophene with Mg to yield the Grignard reagent, followed by reaction with chlorodiphenylphosphine (Scheme 1). Compound **1** could not be crystallized


Scheme 1

DOI: 10.1039/b001898h

J. Chem. Soc., Dalton Trans., 2000, 2729–2737   **2729**
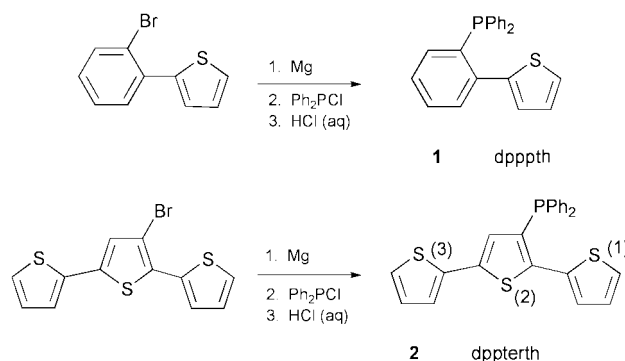
and was isolated as a very thick oil. When stored at 0 °C, the pale yellow product was stable in air for several months. Compound **2** (dpterth) was synthesized by the reaction of 3′-bromo-2,2′ : 5′,2″-terthiophene with *n*-butyllithium followed by reaction with chlorodiphenylphosphine. The product was isolated as a light yellow solid which oxidized slowly in air.

Synthesis and structures of 3 and 4

Ruthenium(II) complexes of dppth and dpterth were prepared by reaction of slightly more than two equivalents of the ligands with [RuCl$_2$(PPh$_3$)$_3$]. Complexes **3** and **4** were
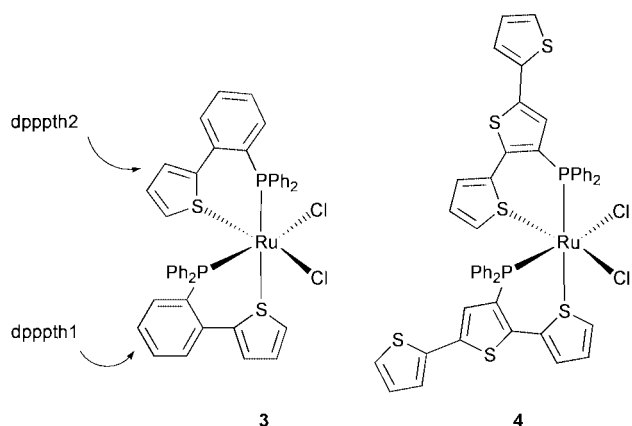
afforded in good yields as microcrystalline rust colored and orange solids, respectively. Both complexes are air stable in the solid state and are soluble in polar organic solvents such as methylene chloride and acetone.

Solutions of **3** in methylene chloride are not stable in air and turn green within 15 min unless kept under nitrogen. The ^{31}P NMR spectrum of **3** consists of two doublets, indicating that the phosphorus centers are in a *cis* arrangement. In addition, a small singlet is observed at δ_P 39.72 indicating the presence of a second structure in solution in which the phosphorus nuclei are equivalent.

Crystals of **3** were grown by slow diffusion of hexanes into a solution of the compound in chloroform. The solid-state structure of **3·3CHCl$_3$** is shown in Fig. 1 and selected bond lengths and angles are presented in Tables 1 and 2. Redissolving these crystals in CDCl$_3$ shows the same ratio of isomers by ^{31}P NMR as before crystallization suggesting that the isomers are in equilibrium in solution. The geometry about the ruthenium is a distorted octahedron where both dppth ligands coordinate in a bidentate fashion *via* the phosphorus and sulfur atoms. Only one enantiomer was found in the crystal structure. Both thiophenes are coordinated to the metal *via* the sulfur in an η^1 binding mode and the two Ru–S bond lengths are in the range reported for ruthenium complexes containing η^1-coordinated thiophene rings.[9–11]

The two dppth ligands are not equivalent in this structure. The phenyl and thienyl rings in the ligand containing P(2) and S(2) (dppth2) are coplanar. In the other ligand (dppth1), the phenyl and thienyl rings are twisted with respect to one another with a dihedral angle of *ca.* 50°. The bite angle (P–Ru–S) of dppth1 is 81.5 and 90.8° for dppth2. The Ru–S bond lengths are within the range reported for η^1-coordinated thiophenes,[9–11] with a shorter bond for the ligand with the thienyl group *trans* to Cl (dppth2). In both ligands, the plane of the thiophene ring is tilted with respect to the Ru–S axis with an angle of 128° for dppth1 and 150° for dppth2 (Table 2). The tilt angle of the thiophene in dppth1 is in the range observed in other ruthenium complexes containing η^1 bound thiophenes.[9–11] To our knowledge, the tilt angle of the thiophene in dppth2 is the largest reported to date for S-coordinated thiophene. It is nearly 20° larger than for [RuCl$_2$(P{dbt}{4-tol}$_2$-*P,S*)$_2$] (tol = tolyl,

Table 1 Selected bond lengths (Å) and angles (°) for **3**

|			
Ru–Cl(1)	2.4676(12)	Ru–Cl(2)	2.4080(12)
Ru–P(1)	2.3191(12)	Ru–P(2)	2.3392(12)
C(4)–C(5)	1.461(7)	P(1)–C(10)	1.857(5)
C(26)–C(27)	1.462(8)	P(2)–C(32)	1.876(5)
Cl(1)–Ru–P(1)	169.62(5)	S(1)–Ru–P(2)	165.93(5)
Cl(2)–Ru–S(2)	178.00(6)	S(1)–Ru–P(1)	90.81(4)
S(2)–Ru–P(2)	81.48(5)	S(1)–Ru–S(2)	95.44(6)
Ru–S(1)–C(1)	115.6(2)	Ru–S(1)–C(4)	111.23(17)
Ru–S(2)–C(23)	131.0(3)	Ru–S(2)–C(26)	119.7(2)
Ru–P(1)–C(10)	115.18(16)	Ru–P(2)–C(32)	110.33(18)
S(1)–C(1)–C(2)	112.8(5)	S(1)–C(4)–C(3)	110.1(4)
C(1)–C(2)–C(3)	112.8(5)	C(2)–C(3)–C(4)	114.1(5)
C(1)–S(1)–C(4)	91.7(3)	S(2)–C(23)–C(24)	106.0(6)
S(2)–C(26)–C(25)	106.7(6)	C(23)–C(24)–C(25)	114.3(8)
C(24)–C(25)–C(26)	113.6(8)	C(23)–S(2)–C(26)	98.8(3)
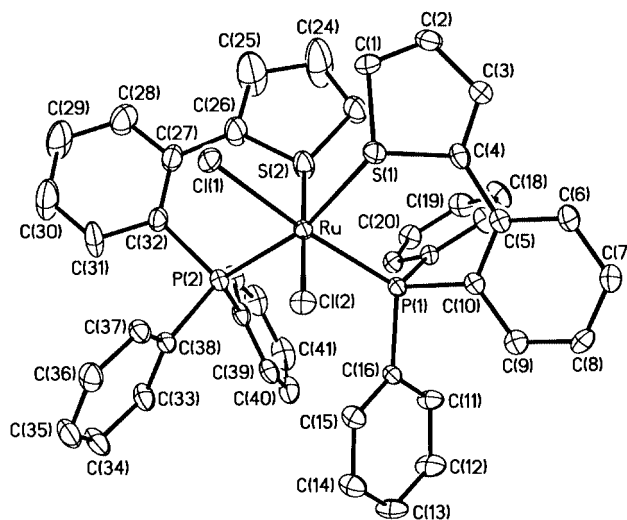
Fig. 1 ORTEP[53] view of **3**. Vibrational ellipsoids are drawn at the 30% probability level.

dbt = dibenzothienyl) (132°)[13] and 10° larger than for [ReCp*-(CO)$_2$(C$_4$H$_4$S)] (140.4°).[34]

In the η^1-coordination mode, thiophene acts primarily as a σ donor, but has also been shown to act as a π acceptor.[35] The extent of π backbonding has been demonstrated to be related to both the ring tilt angle and the Ru–S bond length. In **3**, the thienyl ring in dppth2 has both a shorter Ru–S bond length and a larger tilt angle than in dppth1 indicating that π backbonding is more significant in dppth2. The bond lengths in the coordinated thienyl groups in **3** are different from those in thiophene (Table 2) (*vide infra*).[36]
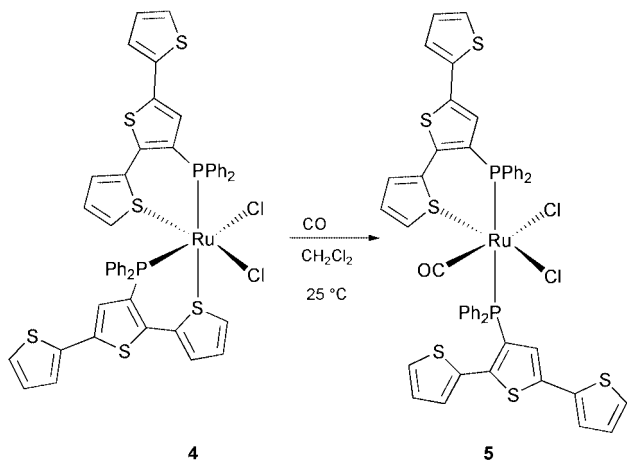
Compound **4** is stable in solution and its ^{31}P NMR spectrum contains a singlet at δ_P 26.96 as well as a pair of doublets. Based on the similarities to the spectrum of **3**, the two doublets are assigned to a *cis* isomer of **4**, and the singlet assigned to a second structure in which the phosphorus nuclei are equivalent. Based on the crystal structure of **3** and the NMR spectra, we assume that the *cis* form of **4** also has an all-*cis* geometry. At room temperature, 60% of the mixture is the *cis* isomer, and all attempts to isolate the isomers were unsuccessful, which suggests that the two species may also be in equilibrium in solution.

Reactions of 3 and 4 with CO

Complexes **3** and **4** both react in solution with carbon monoxide; however, the reaction is slower than with similar complexes containing hemilabile phosphine–ether ligands, such as [RuCl$_2$({2-PPh$_2$}C$_6$H$_4$OCH$_3$-*P,O*)$_2$].[37] The reaction of **4** with carbon monoxide (Scheme 2) results in the formation of

Table 2 Bond lengths and tilt angles of the η^1-coordinated thienyl groups

| Compound | Tilt angle/° | Bond length/Å | | | |
		Ru–S	C–S	C=C	C–C
3/dpppth1	128	2.4106(12)	1.738(4), 1.734(5)	1.343(8), 1.349(7)	1.420(8)
3/dpppth2	150	2.2790(15)	1.671(6), 1.671(6)	1.348(10), 1.361(11)	1.436(12)
5	125	2.340(4)	1.738(13), 1.738(4)	1.353(17), 1.321(15)	1.457(17)
8	153	2.3068(9)	1.728(4), 1.738(4)	1.358(6), 1.364(6)	1.416(6)
Thiophene[a]	—	—	1.714(1)	1.370(2)	1.424(2)

[a] From ref. 36.
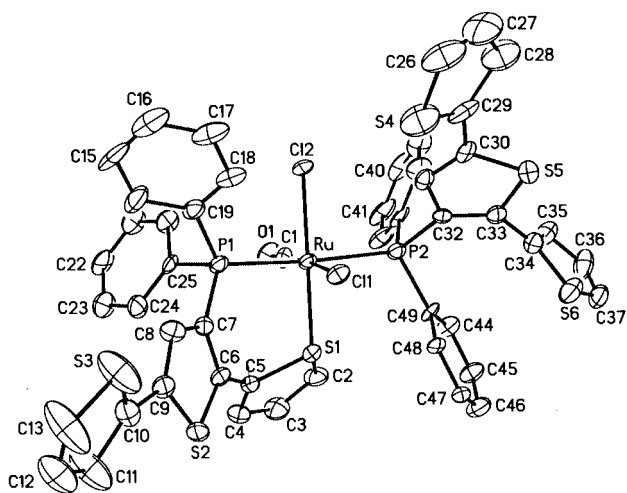
Fig. 2 ORTEP[53] view of **5**. Vibrational ellipsoids are drawn at the 30% probability level.

Scheme 2

Table 3 Selected bond lengths (Å) and angles (°) for **5**

Ru–Cl(1)	2.452(4)	Ru–Cl(2)	2.386(3)
Ru–P(1)	2.367(4)	Ru–P(2)	2.401(4)
Ru–C(1)	1.810(15)	C(1)–O(1)	1.133(13)
P(1)–C(7)	1.816(13)	C(5)–C(6)	1.406(15)
S(2)–C(6)	1.709(13)	C(9)–S(2)	1.709(13)
P(2)–C(32)	1.806(13)	S(5)–S(33)	1.748(13)
S(5)–C(30)	1.702(13)	S(6)–C(34)	1.595(15)
S(6)–C(37)	1.545(16)		
S(1)–Ru–P(1)	91.8(5)	S(1)–Ru–Cl(2)	178.68(13)
P(1)–Ru–P(2)	172.89(13)	Cl(1)–Ru–C(1)	175.0(4)
Ru–C(1)–O(1)	178.4(13)	Ru–P(1)–C(7)	112.8(4)
Ru–P(2)–C(32)	115.9(4)	C(2)–S(1)–C(5)	92.9(7)
S(1)–C(2)–C(3)	110.8(11)	C(2)–C(3)–C(4)	112.3(13)
C(4)–C(5)–S(1)	110.4(11)	C(6)–S(2)–C(9)	92.2(7)

one major product **5** that exhibits two closely spaced resonances at δ_P 5.89 and 5.52. The IR spectrum of this product contains one sharp peak in the carbonyl stretching region at 1973 cm^{-1}.

Crystals of **5·CHCl$_3$** were grown by slow diffusion of hexanes into a chloroform solution of the compound, and the solid-state crystal structure is shown in Fig. 2. Selected bond lengths and angles are collected in Tables 2 and 3. The structure shows that **5** is a monocarbonyl complex with the Ru in a slightly distorted octahedral environment. The two phosphorus atoms are oriented *trans* to each other and the carbonyl is *trans* to one of the chloro ligands while the coordinated thienyl group is *trans* to the other chloro group. The monocarbonyl complex resulting from the reaction of [RuCl$_2$(P{dbt}{4-tol}$_2$-P,S)$_2$] with CO has the same geometry around the ruthenium center as **5**.[38] The ^{31}P NMR spectrum of **5** consists of an AB spin pattern where the difference in chemical shift is very small. Only the

inner peaks of the two doublets are observed and the chemical shift difference between the peaks increases with magnetic field, consistent with this assignment.

Although **4** exists as a mixture of isomers in solution, only one product **5** results from the reaction with CO. This suggests a reaction pathway that involves isomerization of the reactants prior to reaction with CO. There is no evidence for the formation of dicarbonyl complexes even when **4** is left to react with CO for three days at 25 °C. The thiophene *trans* to the chloro in **5** may be too strongly coordinated to be displaced by a second CO under these conditions.

Compound **5** contains both bidentate and monodentate forms of dppterth; thus, it is possible to compare the bond lengths and angles of both forms of the ligand in a single structure. The bidentate dppterth ligand forms a six-membered ring with a bite angle (P–Ru–S) of 91°. In this ligand, the Ru–S bond length for the η^1-bound thienyl ring is 2.340(4) Å, which is comparable to the Ru–S bond lengths in **3**. The thiophene plane in **5** is tilted with respect to the Ru–S axis with an angle of 125°, comparable to the tilt angle in dpppth1 in **3**, suggesting that there is a comparable degree of backbonding in these thiophene–Ru bonds. Despite their different coordination modes, there are only slight differences in bond lengths and angles between the two dppterth ligands and these are close to those observed in the structure of 3'-methyl-2,2':5',2''-terthiophene.[39] The bond lengths of the coordinated thienyl group in **5** are similar to those observed for the dpppth1 ligand in **3** (Table 2). The coordination of the sulfur of one of the rings in the terthienyl moiety to the Ru does not introduce any major perturbations in the structure of the oligomer.

When **3** reacts with CO, two major products are formed, both of which appear as singlets (δ_P 17.7 and 10.9) in the ^{31}P NMR spectrum. The mixture of the two products has three absorption bands in the carbonyl stretching region of the IR spectrum, at 1976, 2015 and 2098 cm^{-1}. By comparison with **5** (ν_{CO} = 1973 cm^{-1}), we assign one product as the monocarbonyl **6** (ν_{CO} = 1976 cm^{-1} and δ_P 17.7) (Scheme 3). The second product is assigned as the *cis* dicarbonyl **7** (ν_{CO} = 2015 and 2098 cm^{-1} and δ_P 10.9) by comparison to the IR spectrum of the closely related dicarbonyl [RuCl$_2$(CO)$_2$(PPh$_3$)$_2$].[40]

Table 4 81.015 MHz $^{31}P\{^1H\}$ NMR ^{a} data for complexes with AMX spin pattern

		δ			J/Hz		
Complex		P_A	P_M	P_X	$^2J_{AM}$	$^2J_{AX}$	$^2J_{MX}$
8	*cis*-[RuCl$_2$(dppm)(dppterth-*P*,*S*)]	4.88	−10.64	−23.73	24.5	41.3	363
9	*trans*-[RuCl$_2$(dppm)(dppterth-*P*,*S*)]	16.11	−2.74	−14.99	27.5	61.2	322
10	*trans*-[RuCl$_2$(CO)(dppm)(dppterth-*P*)]	10.18	−8.19	−20.56	21.0	42.7	364
11	*cis*-[RuCl$_2$(CO)(dppm)(dppterth-*P*)]	−40.76	2.97	−9.30	27.8	33.4	273

^{a} Solvent: CDCl$_3$.
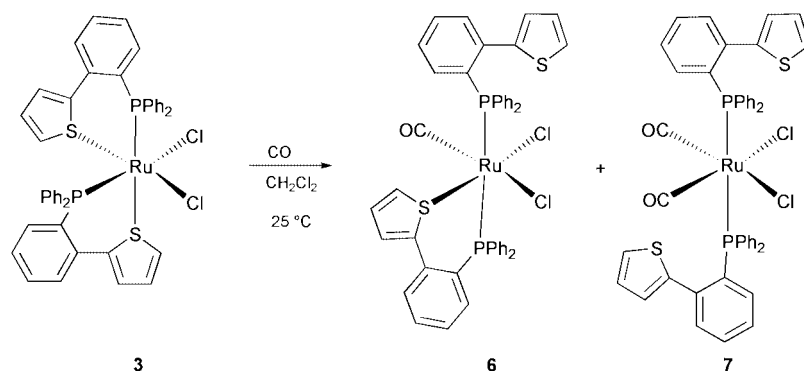
Scheme 3

Solutions of **7** are not stable in air and convert to **6** by loss of CO, shown by the disappearance of the absorption at 2098 cm^{-1} and the concomitant growth of the band at 1976 cm^{-1}. All attempts to precipitate the reaction products under a CO atmosphere yielded mixtures with **6** as the dominant species. Efforts to purify **6** by bubbling N$_2$ through a mixture of **6** and **7** to remove the latter were unsuccessful owing to the presence of several side-products which could not be separated. Similarly, when N$_2$ is bubbled through a solution of **6** for 12 h in an effort to decarbonylate completely to **3**, the ^{31}P NMR spectrum of the resulting reaction mixture is very complicated, showing **3** as a minor product along with several resonances that could not be assigned to any known compounds.

Synthesis and structure of 8 and 9

Treatment of a solution of **4** with one equivalent of bis(diphenyl-phosphino)methane (dppm) at room temperature results in the displacement of one of the dppterth ligands to yield complex **8**
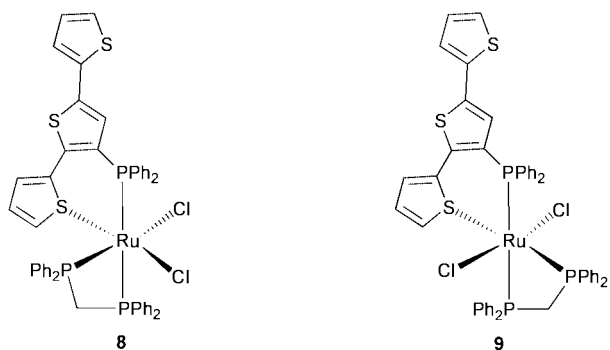
and a small amount of *trans*-[RuCl$_2$(dppm)$_2$]. The ^{31}P NMR spectrum of **8** consists of an AMX coupling pattern, and this data is shown in Table 4. The assignment of the phosphorus resonances is shown in Scheme 5.

Crystals of complex **8**·3CH$_2$Cl$_2$ were obtained by slow diffusion of hexanes into a solution of the compound in methylene chloride. The solid-state structure is shown in Fig. 3 and
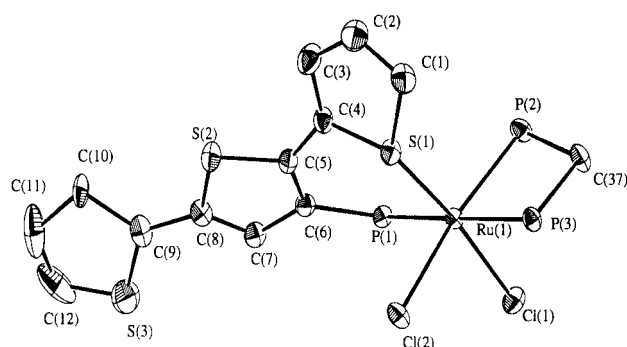
Fig. 3 ORTEP[53] view of **8**. Vibrational ellipsoids are drawn at the 30% probability level. Phenyl groups have been omitted for clarity.

selected bond lengths and angles are shown in Tables 2 and 5. In this structure, the ruthenium center is in a distorted octahedral environment, due to the small bite angle (P–Ru–P) of the dppm ligand. The chloro ligands are in a *cis* arrangement, and the dppterth ligand chelates to form a six-membered ring with a bite angle (P–Ru–S) close to 90°. Dppterth can form either a six- or seven-membered ring depending on which terminal thiophene in the terthienyl group is coordinated; however, we do not see any evidence for formation of the seven-membered ring isomer in **8**. The thiophene is coordinated through the sulfur atom with a Ru–S bond length of 2.3068(9) Å and a tilt angle of 153°. This angle is even larger than the tilt angle of dpppth2 in **3** indicating that the extent of π backbonding to the thiophene in **8** is much larger than in **5** and comparable to dpppth2 in **3**. The bond lengths in the coordinated thienyl ring in **8** are comparable to those in dpppth1 in **3** and in **5** (Table 2). Overall, the terthienyl group in **8** is only slightly distorted with respect to the structure of 3′-methyl-2,2′ : 5′,2″-terthiophene.[39]

It has been suggested that π backbonding with coordinated thiophene rings should result in a slight weakening of the C–S bonds in the ring.[35] We observe this in all the structures in this work with the exception of dpppth2 in **3**. Despite a large tilt angle, the C–S bonds in this ligand are shorter than the C–S bonds in thiophene (Table 2). At this time we do not have an explanation for this anomaly.

Table 5 Selected bond lengths (Å) and angles (°) for **8**

|			
Ru–Cl(1)	2.4060(9)	Ru–Cl(2)	2.4854(9)
Ru–P(1)	2.3861(9)	Ru–P(2)	2.3122(9)
Ru–P(3)	2.3336(9)	C(4)–C(5)	1.442(5)
P(1)–C(6)	1.825(4)	C(8)–C(9)	1.448(5)
Cl(1)–Ru–S(1)	172.80(4)	Cl(2)–Ru–P(2)	165.92(3)
P(1)–Ru–P(3)	174.43(3)	S(1)–Ru–P(1)	90.33(3)
P(2)–Ru–P(3)	72.27(3)	Ru–S(1)–C(4)	121.6(1)
Ru–S(1)–C(1)	131.7(1)	S(1)–C(1)–C(2)	109.9(3)
Ru–P(1)–C(6)	114.5(1)	C(2)–C(3)–C(4)	113.7(4)
S(1)–C(4)–C(3)	109.3(3)	S(1)–C(4)–C(5)	120.3(3)
C(1)–C(2)–C(3)	113.7(4)		

In the reaction of **4** with dppm, only one isomer **8** forms. It is possible that this reaction proceeds *via* a two-step pathway, in which the first step is dissociation of the thiophene end of one of the dppterth ligands, followed by the monodentate coordination of dppm. The second step would then involve loss of the monodentate dppterth and the chelation of dppm. It is interesting that one of the two dppterth ligands in **4** is preferentially displaced by dppm to yield only the isomer **8**. We infer from the structure of **3** that the degree of π backbonding and consequently the lability of the two dppterth ligands in **4** is likely quite different. The second dppterth ligand in **4** can eventually be displaced by dppm, as evidenced by the small amount of *trans*-[RuCl₂(dppm)₂] that forms.

When a solution of **8** is left in ambient laboratory light at room temperature, the complex slowly isomerizes to **9** and reaches equilibrium at a ratio close to 1:1. Under identical conditions, **9** also slowly isomerizes to **8**, reaching the same equilibrium. The complex **9** can be isolated by passing the mixture through a column of neutral alumina, and the ³¹P NMR spectrum of this compound also consists of an AMX coupling pattern (Table 4). The ³¹P NMR coupling constants for **9** indicate a meridional arrangement of the phosphorus atoms;[41] therefore, the only possible structure for **9** that is consistent with this data is the isomer in which the chloro groups are *trans*.

Reactions of 8 and 9 with CO

Complex **8** reacts slowly with CO in solution at room temperature (Scheme 4). The reaction vessel was kept in the dark to prevent isomerization of the starting material to **9** and approximately 30% conversion to the monocarbonyl **10** is achieved after 14 h. This complex was separated from the reaction mixture by chromatography on a column of neutral alumina. Complex **9** also reacts with CO at −8 °C in the dark to yield a different monocarbonyl complex **11**. These conditions were necessary to prevent the isomerization of the starting material to **8** and in this case, the conversion was complete after 14 h. Compounds **10** and **11** both have an AMX coupling pattern in their ³¹P NMR spectra (Table 4) and their IR spectra contain single sharp bands in the carbonyl stretching region at 2020 and 1975 cm⁻¹, respectively.

The structures of **10** and **11** (Scheme 4) are assigned based on the IR and ³¹P NMR spectral data for those compounds. By comparison to the number and position of the bands in the far-IR spectra of related complexes,[42] the RuCl₂ stretching frequencies indicate that the chloro group are *trans* in **10** and *cis* in **11**. The coupling constants (J_{PP}) in the ³¹P NMR spectra show that the phosphorus atoms in both complexes are in a meridional arrangement around the metal.[41] In **10**, P_A is shifted upfield due to the *trans* carbonyl group, and similar shifts have been observed in the *trans* isomers of complexes such as [RuCl₂(PR₃)₃(CO)] (PR₃ = PMe₃, PPhMe₂ and PPh₂Me).[43] The carbonyl stretching frequency for **10** (1975 cm⁻¹) is in the range observed for closely related complexes in which CO is *trans* to Cl such as **5** (1973 cm⁻¹) and [RuCl₂(AsPh₃)₃(CO)] (1961
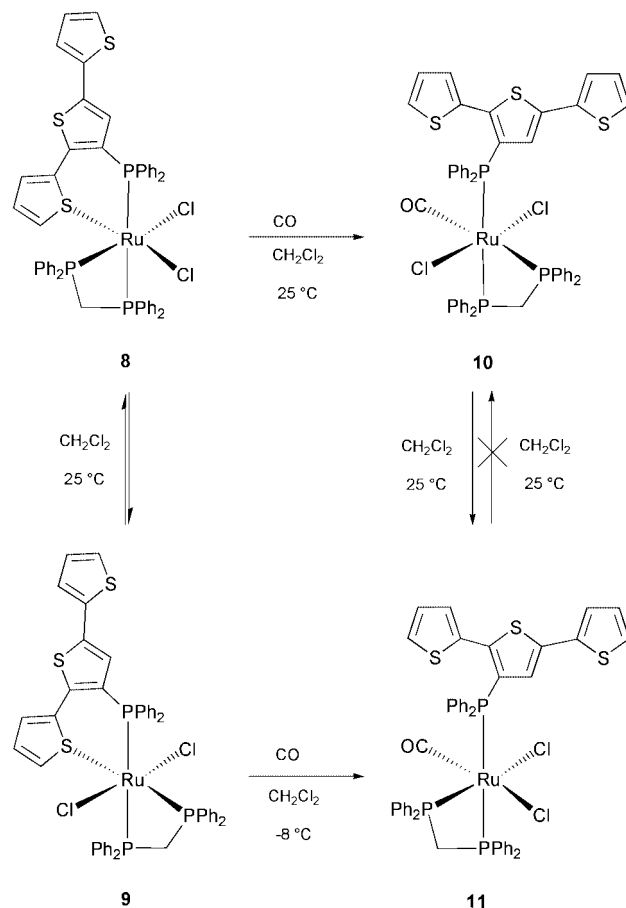
Scheme 4

cm⁻¹),[40] while the CO stretching frequency for **11** (2020 cm⁻¹) is consistent with a *trans* phosphorus ([RuCl₂(PPh₂Me)₃(CO)], 1991 cm⁻¹).[43]

At room temperature, **10** is thermally converted to the isomer **11**, without formation of **8** or **9** (Scheme 4). The reverse reaction (**11** to **10**) does not proceed at room temperature in ambient light. Similar isomerizations have been reported for related complexes such as [RuCl₂(PR₃)₃(CO)] (PR₃ = PMe₃, PPhMe₂ and PPh₂Me).[43] In ruthenium(II) complexes containing carbonyl ligands, the thermodynamic stability is directed in part by the nature of the ligand found *trans* to the carbonyl group. Since CO is a strong π-acceptor, any *trans* ligand competing for electron density from the metal center will weaken the M–CO bond and this *trans* influence decreases in the order CO > P > Cl.[44] Thus, complexes containing a chloro *trans* to a carbonyl are thermodynamically more stable than isomers with either a phosphine or a CO *trans* to a carbonyl, as reported in the literature.[43,45,46]

When **8** reacts with CO at room temperature, only **10** forms while the reaction of **9** with CO yields only **11**. It is possible that **10** forms *via* a pentacoordinate intermediate resulting from dissociation of the thiophene sulfur (Scheme 5). Such intermediates have been proposed in many displacement reactions involving Ru complexes containing hemilabile ligands.[47,48] The CO then reacts on the less hindered face of the bipyramidal intermediate, which would yield the observed product. The reaction of **9** with CO probably proceeds *via* a different intermediate than for **8** since the product is not the same. One possibility is a pathway involving an intermediate in which the Ru–S bond weakens but does not completely dissociate when the CO approaches, due to the lower temperature of this reaction. The thiophene only fully dissociates when the CO reacts with the face which yields the more stable product, with the chloro group *trans* to the CO. Further experiments to fully elucidate these reaction mechanisms are needed.

Table 6 UV–VIS spectral data

	Complex	UV–VIS λ_{max}/nm (ε/M^{-1} cm^{-1})[a]
1	dpppth	228 (2.14 × 10^4), 266 (1.66 × 10^4)
2	dppterth	254 (2.08 × 10^4), 354 (1.77 × 10^4)
3	[RuCl$_2$(dpppth-*P,S*)$_2$]	318 (sh) (1.73 × 10^4), 356 (sh) (7.32 × 10^3), 484 (sh) (9.5 × 10^2)
4	[RuCl$_2$(dppterth-*P,S*)$_2$]	356 (br) (2.13 × 10^4)
8	*cis*-[RuCl$_2$(dppm)(dppterth-*P,S*)]	322 (1.17 × 10^4), 374 (1.78 × 10^4), 510 (1.10 × 10^3)
9	*trans*-[RuCl$_2$(dppm)(dppterth-*P,S*)]	316 (sh) (1.14 × 10^4), 382 (1.48 × 10^4), 518 (2.91 × 10^2)
5	[RuCl$_2$(CO)(dppterth-*P*)(dppterth-*P,S*)]	238 (1.22 × 10^5), 254 (sh) (1.17 × 10^5), 286 (sh) (8.21 × 10^4), 346 (6.65 × 10^4)
6	[RuCl$_2$(CO)(dpppth-*P*)(dpppth-*P,S*)]	252 (sh) (1.11 × 10^5), 308 (sh) (3.19 × 10^4), 390 (sh) (3.25 × 10^3)
10	*cis*-[RuCl$_2$(CO)(dppm)(dppterth-*P*)]	276 (sh) (2.66 × 10^4), 340 (1.37 × 10^4)
11	*trans*-[RuCl$_2$(CO)(dppm)(dppterth-*P*)]	246 (sh) (8.68 × 10^4), 336 (4.07 × 10^4)

[a] Solvent: CH$_2$Cl$_2$; sh = shoulder; br = broad.
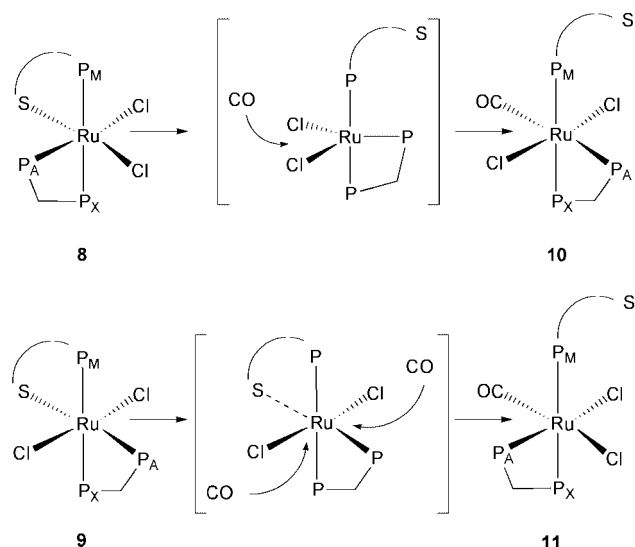
Scheme 5

Electronic spectra

The UV–VIS spectral data for all the complexes are shown in Table 6. Compound **1** has an absorption in the UV region at 266 nm, which is comparable in position and intensity to the π–π* transition of 2-phenylthiophene (282 nm).[49] The free ligand dppterth has an absorption at 354 nm, similar to the π–π* transition of terthiophene (351 nm).[49] In complex **3**, high energy bands can be observed in the UV region of the spectrum along with a weak band at 484 nm. The latter is assigned to a Ru d–d transition and the higher energy bands to ligand-based π–π* transitions. The spectrum of complex **4** contains a broad band with a maximum at 356 nm. Since the complex is present in solution as a mixture of two isomers, it is likely that the absorption bands of the two species overlap and cannot be resolved.

The spectra of **8** and **9** are very similar to one another, both showing high energy bands which are due to ligand-based π–π* transitions. A small red-shift is observed for these absorptions relative to dppterth, which can be attributed to electronic or steric effects in the terthienyl fragment of dppterth. Comparison of the bond lengths and angles of dppterth in **8** with those of 3′-methyl-2,2′:5′,2″-terthiophene[39] shows that the structure of the terthienyl moiety is only slightly perturbed. The red-shift is, therefore, due to a combination of two factors: (a) electron donation from the metal to the terthienyl group and (b) a more rigid backbone in the coordinated oligomer. It has been reported that the absorption bands of thiophene oligomers with rigid backbones are red-shifted owing to the reduction in rotational disorder relative to less rigid analogs.[50]

The weak bands at 510 nm in **8** and 518 nm in **9** are assigned to d–d transitions.

Upon reaction of the complexes with CO, substantial changes occur in the electronic spectra. In the spectrum of complex **5**, multiple overlapping bands are observed, and it is likely that the different electronic transitions are due to the two coordination modes of the two dppterth ligands. The spectrum of **6** (also containing **7** and other impurities) shows only poorly resolved UV absorptions tailing into the visible. In the spectrum of **10** and **11**, the d–d band observed in **8** and **9** at *ca.* 500 nm is absent. The higher energy bands are assigned to ligand-based π–π* transitions. In both complexes, the ligand absorptions are blue-shifted with respect to **8** and **9**. This is due to the reduction of electron donation from the Ru and removal of the rigidity in the terthienyl moiety when dppterth is monodentate. The ligand-based absorptions of **10** and **11** are also slightly blue-shifted with respect to dppterth. This may be due to a small electron withdrawing effect of the ruthenium carbonyl group in **10** and **11**.

Experimental

General

2-(2′-Bromophenyl)thiophene,[54] 3′-bromo-2,2′:5′,2″-terthiophene[55] and [RuCl$_2$(PPh$_3$)$_3$][40] were all prepared according to literature procedures. Diethyl ether and THF were distilled from sodium/benzophenone; methylene chloride was distilled from CaCl$_2$. All other reagents were purchased from either Aldrich or Strem Chemicals and used as received. Electronic absorption spectra were obtained on an UNICAM UV-2 spectrometer. IR spectra were obtained on a Bomem MB-series spectrometer on either methylene chloride solutions or caesium iodide pellets. ^{1}H and ^{31}P NMR experiments were performed on either a Bruker AC-200E or a Varian XL-300 spectrometer, and spectra were referenced to residual solvent (^{1}H) or external 85% H$_3$PO$_4$ (^{31}P).

Preparations

2-(2′-{Diphenylphosphino}phenyl)thiophene (dpppth) 1. 2-(2′-Bromophenyl)thiophene (7.70 g, 32.2 mmol) and Mg (0.850 g, 35.4 mmol) were added to dry THF (45 mL) at 60 °C and allowed to react for 1 h at room temperature after which time chlorodiphenylphosphine (7.71 g, 35.0 mmol) was added dropwise. The reaction mixture was stirred for 1 h and was then quenched with 0.5 M HCl (100 mL). The organic layer was washed with water, dried over anhydrous MgSO$_4$ and the solvent removed *in vacuo* to yield the crude product, which was purified by chromatography on silica gel with a hexanes–acetone mixture (98/2 v/v). The yellow band was collected and the solvent removed, leaving pure **1** as a thick yellow oil. Yield: 7.90 g (71%). ^{1}H NMR (200 MHz, CDCl$_3$): δ 7.57–7.46

(m, 1H), 7.44–7.18 (m, 13H), 7.08–6.82 (m, 3H). $^{31}P\{^1H\}$ NMR (81.015 MHz, CDCl$_3$): δ −15.13. Anal. C$_{22}$H$_{17}$PS requires C, 76.74; H, 4.94. Found: C, 76.83; H, 4.95%.

3′-Diphenylphosphino-2,2′:5′,2″-terthiophene (dppterth) 2. A solution of *n*-butyllithium in hexanes (1.6 M, 0.38 mL, 0.61 mmol) was added dropwise to a solution of 3′-bromo-2,2′:5′,2″-terthiophene (0.20 g, 0.61 mmol) in dry diethyl ether (7 mL) at −15 °C. The mixture was stirred for 1 h at −15 °C and then allowed to warm to room temperature. A solution of chlorodiphenylphosphine (0.14 g, 0.62 mmol) in diethyl ether was then added dropwise. The resulting solution was stirred for another 30 min at room temperature, after which time 1 M HCl (25 mL) was added to quench the reaction. The organic layer was washed with water, dried over anhydrous MgSO$_4$ and the solvent removed to yield an oily solid. The crude solid was purified by chromatography on silica gel using a hexanes–acetone mixture (8/2 v/v) as eluant. The yellow band was collected and the solvent removed to give a solid, which was dissolved in a small amount of methylene chloride to which hexanes were added to yield **2** as a yellow powder. Yield: 0.20 g (76%). ^1H NMR (200 MHz, CDCl$_3$): δ 7.36 (m, 10H), 7.29 (m, 1H), 7.17 (m, 2H), 7.07 (m, 1H), 6.98 (m, 2H), 6.06 (m, 1H). $^{31}P\{^1H\}$ NMR (81.015 MHz, CDCl$_3$): δ −25.79. Anal. C$_{24}$H$_{17}$PS$_3$ requires C, 66.67; H, 3.94. Found: C, 66.05; H, 4.01%.

[RuCl$_2$(dpppth-*P*,*S*)$_2$] 3. [RuCl$_2$(PPh$_3$)$_3$] (1.00 g, 1.04 mmol) and **1** (1.08 g, 3.13 mmol) were added to dry methylene chloride (60 mL) under a N$_2$ atmosphere. After the reaction mixture was stirred at room temperature for 13 h, the solvent was removed. The resulting solid was extracted with diethyl ether to leave a red powder which was collected. The crude product was dissolved in methylene chloride and a small amount of hexanes added until a fine gray precipitate appeared. The residual solution was filtered off and the gray precipitate was discarded. More hexanes were added to the mother-liquor to precipitate the product as a rust colored powder. The product was isolated as a mixture of *cis* and *trans* isomers. Yield: 0.68 g (76%). ^1H NMR (200 MHz, CDCl$_3$): δ 8.00–8.12 (m, 2H), 7.80–7.31 (m, 12H), 7.28–7.00 (m, 8H), 6.92–6.40 (m, 9H), 6.00–6.08 (m, 2H), 5.67–5.75 (m, 1H). $^{31}P\{^1H\}$ NMR (81.015 MHz, CDCl$_3$): δ 36.36 (d, 1P, J_{PP} = 160 Hz), 34.83 (d, 1P, J_{PP} = 160 Hz), 39.72 (s). Anal. C$_{44}$H$_{34}$Cl$_2$P$_2$S$_2$Ru requires C, 61.39; H, 3.95. Found: C, 61.71; H, 4.23%.

[RuCl$_2$(dppterth-*P*,*S*^{1})$_2$] 4. [RuCl$_2$(PPh$_3$)$_3$] (1.8 g, 1.9 mmol) and **2** (2.0 g, 4.6 mmol) were added to dry methylene chloride (80 mL) under a N$_2$ atmosphere. After the reaction mixture was stirred at room temperature for 15 h, the solvent was removed and the resulting solid extracted with diethyl ether to leave a dark orange powder which was collected. The crude product was dissolved in a small amount of methylene chloride and hexanes added to precipitate the product as an orange powder. The product was isolated as a mixture of isomers. Yield: 1.9 g (97%). ^1H NMR (200 MHz, CDCl$_3$): δ 8.21–7.96 (m, 3H), 7.80–6.78 (m, 28H), 6.68–5.92 (m, 3H). $^{31}P\{^1H\}$ NMR (81.015 MHz, CDCl$_3$): δ 23.89 (d, 1P, J_{pp} = 137 Hz), 22.75 (d, 1P, J_{pp} = 137 Hz), 26.94 (s). Anal. C$_{48}$H$_{34}$Cl$_2$P$_2$S$_6$Ru requires C, 55.60; H, 3.28. Found: C, 55.33; H, 3.30%.

***cis*-[RuCl$_2$(dppm)(dppterth-*P*,*S*^{1})] 8.** Bis(diphenylphosphino)-methane (dppm) (0.371 g, 0.965 mmol) was added to a solution of **4** (1.00 g, 0.965 mmol) in dry methylene chloride (50 mL). The mixture was stirred at room temperature for 10 h after which time the solvent was removed *in vacuo*. The resulting solid was purified by chromatography on neutral alumina. The column was first eluted with methylene chloride to remove excess dppm, dppterth and *trans*-[RuCl$_2$(dppm)$_2$] until the eluent was colorless, then the product eluted as a red band with

a mixture of acetone and methylene chloride (2/3 v/v). Removal of the solvent and crystallization from methylene chloride–hexanes yielded pure **8** as a red powder. Yield: 0.70 g (73%). ^1H NMR (200 MHz, CDCl$_3$): δ 8.22–8.30 (m, 2H), 7.94–8.02 (m, 4H), 7.50–6.60 (m, 28H), 6.55 (d, 1H), 6.16–6.24 (m, 1H), 5.18 (d, 1H), 4.98–5.06 (m, 1H), 4.64–4.70 (m, 1H). FIR (CsI): v_{as}(RuCl$_2$) = 319 cm^{-1}, v_s(RuCl$_2$) = 271 cm^{-1}. Anal. C$_{49}$H$_{39}$Cl$_2$P$_3$S$_3$Ru requires C, 59.50; H, 3.95. Found: C, 59.22; H, 3.98%.

***trans*-[RuCl$_2$(dppm)(dppterth-*P*,*S*^{1})] 9.** A solution of **8** (556 mg, 0.560 mmol) in dry methylene chloride (30 mL) was stirred at room temperature for 24 h in ambient room light. The mixture was then eluted on a neutral alumina column with methylene chloride and the red–brown band collected. Removal of the solvent and recrystallization from methylene chloride–hexanes yielded **9** as a rust colored powder. Unreacted **8** was recovered by washing the column with an acetone–methylene chloride mixture (2/3 v/v). Yield: 150 mg (27%). ^1H NMR (200 MHz, CDCl$_3$): δ 7.56–7.64 (m, 4H), 7.40–6.85 (m, 32H), 6.42 (d, 1H), 4.74–4.82 (m, 2H). FIR (CsI): v_{as}(RuCl$_2$) = 325 cm^{-1}. Anal. C$_{49}$H$_{39}$Cl$_2$P$_3$S$_3$Ru requires C, 59.50; H, 3.95. Found: C, 59.26; H, 4.12%.

[RuCl$_2$(CO)(dppterth-*P*)(dppterth-*P*,*S*^{1})] 5. Carbon monoxide was bubbled through a solution of **4** (200 mg, 0.190 mmol) in methylene chloride. After 4 h, the orange solution turned dark orange–yellow, and the flask was sealed and left overnight under a CO atmosphere. The resulting bright yellow mixture was concentrated to 1–2 mL and hexanes were added to precipitate a yellow powder. This solid was dissolved in methylene chloride under CO and hexanes were added yielding **5** as a yellow powder. Yield: 128 mg (58%). ^1H NMR (200 MHz, CDCl$_3$): δ 8.80 (m, 1H), 8.40–7.73 (m, 10H), 7.61–6.76 (m, 19H), 6.64–6.25 (m, 3H), 5.9–5.73 (m, 1H). $^{31}P\{^1H\}$ NMR (81.015 MHz, CDCl$_3$): δ 5.89 (s), 5.52 (s). IR (CH$_2$Cl$_2$): v_{CO} = 1973 cm^{-1}. Anal. C$_{49}$H$_{34}$Cl$_2$OP$_2$S$_6$Ru requires C, 55.26; H, 3.20. Found: C, 54.79; H, 3.50%.

***trans*-[RuCl$_2$(CO)(dppm)(dppterth-*P*)] 10.** In a foil-wrapped reaction flask, carbon monoxide was bubbled through a solution of **8** (190 mg, 0.190 mmol) in methylene chloride for 4 h, then the mixture was left under a CO atmosphere overnight. The resulting orange solution was concentrated to 2–3 mL by blowing CO over the solution and then filtered through a short neutral alumina column. To remove residual **8**, the column was first washed thoroughly with ethyl acetate until the eluent was colorless. A bright yellow band left on the top of the column was then eluted with neat methanol. Removal of the solvent left a yellow powder which was recrystallized from methylene chloride–hexanes at −8 °C. Pure **10** was collected as a yellow powder which was dried under vacuum. Yield: 55 mg (28%). ^1H NMR (200 MHz, CDCl$_3$): δ 7.86 (m, 1H), 7.72–7.96 (m, 33H), 6.76 (m, 3H), 6.62 (d, 1H), 5.16 (d, 1H). IR (CH$_2$Cl$_2$): v(CO) = 2020 cm^{-1}. FIR (CsI): v_{as}(RuCl$_2$) = 326 cm^{-1}. Anal. C$_{50}$H$_{39}$Cl$_2$OP$_3$S$_3$Ru requires C, 59.05; H, 3.84. Found: C, 58.78; H, 4.03%.

***cis*-[RuCl$_2$(CO)(dppm)(dppterth-*P*)] 11.** Carbon monoxide was bubbled through a solution of **9** (200 mg, 0.193 mmol) in methylene chloride (4–5 mL) for 20 min. The flask was then sealed and left overnight in the dark at −8 °C, during which time the mixture changed from orange–red to yellow. Hexanes were added to precipitate a yellow solid which was collected and recrystallized from methylene chloride–hexanes at −8 °C. The pure product was obtained as yellow crystals which were dried under vacuum. Yield: 145 mg (71%). ^1H NMR (200 MHz, CDCl$_3$): δ 8.21–8.01 (m, 2H), 7.96–7.56 (m, 8H), 7.49–6.8 (m, 26H), 6.71 (d, 1H), 6.42–6.32 (m, 1H), 5.00–4.56 (m, 1H).

Table 7 Crystallographic data for **3**, **5** and **8**

	3·3CHCl₃	**5·CHCl₃**	**8·3CH₂Cl₂**
Formula	$C_{47}H_{37}Cl_{11}P_2RuS_2$	$C_{50}H_{35}Cl_5OP_2RuS_6$	$C_{52}H_{45}Cl_8P_3RuS_3$
M	1218.85	1184.40	1243.72
T/K	213(2)	238(2)	173.2
Crystal system	Orthorhombic	Monoclinic	Monoclinic
Space group	$P2_12_12_1$	$P2_1/n$	$P2_1/n$
$a/\text{Å}$	11.1896(8)	17.069 (7)	15.7595(6)
$b/\text{Å}$	19.063(1)	12.857(7)	15.5059(5)
$c/\text{Å}$	23.732(2)	24.092(7)	22.323(1)
$\beta/°$		105.325(9)	93.506(3)
$V/\text{Å}^3$	5062.0(6)	5099.4	5444.8(3)
Z	4	4	4
Refl. collected/unique	12164/8639	4244/2354	11329/9328
$R_1{}^a$	0.0486	0.0621	0.076
$wR_2{}^b$	0.1225	0.1584	0.129

^{a} $R = \Sigma \left| \left| F_o \right| - \left| F_c \right| \right| / \Sigma |F_o|$ (observed data). ^{b} $wR_2 = (\Sigma(F_o{}^2 - F_c{}^2)^2/\Sigma w(F_o{}^2)^2)^{\frac{1}{2}}$ (all data).

IR (CH_2Cl_2): $\nu(CO) = 1975$ cm^{-1}. FIR (CsI): $\nu_{as}(RuCl_2) = 301$ cm^{-1}, $\nu_s(RuCl_2) = 273$ cm^{-1}. $C_{50}H_{39}Cl_2OP_3S_3Ru$ requires C, 59.05; H, 3.84. Found: C, 58.77; H, 4.06%.

X-Ray crystallographic analysis

Suitable crystals of **3** and **5** were selected and mounted on thin, glass fibers using paraffin oil. Data were collected on a Bruker AX SMART 1k CCD diffractometer using 0.3° ω-scans at 0, 90 and 180° in φ at −60 °C for **3** and −35 °C for **5**. The Flack parameter for **3** was refined to nil, which indicates that the true hand of the data has been determined correctly. Three of the thiophene rings in **5** were disordered; however, because of the close proximity of the atomic positions of the contributing disordered rings, only the disordered sulfur atoms could be located with a refined site occupancy distribution of 90/10, 85/15, and 70/30. All scattering factors and anomalous dispersion factors are contained in the SHEXTL 5.10 program library.[51]

A crystal of **8** was mounted on a glass fiber, and data were collected at −100 °C on a Rigaku/ADSC CCD area detector in two sets of scans ($\psi = 0.0–190.0°$, $\chi = 90°$ and $\omega = −18.0$ to 23.0, $\chi = −90°$), using 0.50° oscillations with 27.0 s exposures. All calculations were performed using the teXsan[52] crystallographic software package of the Molecular Structure Corporation. The uncoordinated thiophene is disordered by rotation about the C(8)–C(9) bond causing S(3) and C(10) to exchange positions. Subsequent refinement of the occupancies of S(3) and C(10) led to values of 0.69 and 1.9, respectively, which corresponds to 0.5 S and 0.5 C at each site. Crystallographic data are shown in Table 7.

CCDC reference number 186/2045.

See http://www.rsc.org/suppdata/dt/b0/b001898h/ for crystallographic files in .cif format.

Acknowledgements

References

1 D. D. C. Bradley, *Adv. Mater.*, 1992, **4**, 756.
2 G. Horowitz, *Adv. Mater.*, 1990, **2**, 287.
3 R. P. Kingsborough and T. M. Swager, *Prog. Inorg. Chem.*, 1999, **48**, 123.
4 C. L. Jones and S. J. Higgins, *J. Mater. Chem.*, 1999, **9**, 865.
5 Y. Zhu, O. Clot, M. O. Wolf and G. P. A. Yap, *J. Am. Chem. Soc.*, 1998, **120**, 1812.
6 Y. Zhu and M. O. Wolf, *Chem. Mater.*, 1999, **11**, 2995.
7 Y. Zhu, D. B. Millet, M. O. Wolf and S. J. Rettig, *Organometallics*, 1999, **18**, 1930.
8 C. S. Slone, D. A. Weinberger and C. A. Mirkin, *Prog. Inorg. Chem.*, 1999, **48**, 233.
9 R. J. Angelici, *NATO ASI Series, Ser. 3*, 1998, **60**, 89.
10 R. J. Angelici, *Bull. Soc. Chim. Belg.*, 1995, **104**, 265.
11 T. B. Rauchfuss, *Prog. Inorg. Chem.*, 1991, **39**, 259.
12 D. A. Weinberger, T. B. Higgins, C. A. Mirkin, L. M. Liable-Sands and A. L. Rheingold, *Angew. Chem., Int. Ed.*, 1999, **38**, 2565.
13 T. B. Rauchfuss, S. M. Bucknor, M. Draganjac, C. Ruffig, W. C. Fultz and A. L. Rheingold, *J. Am. Chem. Soc.*, 1984, **106**, 5379.
14 M. Draganjac, C. Ruffig and T. B. Rauchfuss, *Organometallics*, 1985, **4**, 1909.
15 J. Amarasekera and T. B. Rauchfuss, *Inorg. Chem.*, 1989, **28**, 3875.
16 S. Ng, K. Mok and B. Chen, *J. Chem. Soc., Dalton Trans.*, 1998, **23**, 4035.
17 R. Mathieu, M. Alvarez and N. Lugan, *Inorg. Chem.*, 1993, **32**, 5652.
18 R. Mathieu, M. Alvarez, N. Lugan and B. Donnadieu, *Organometallics*, 1995, **14**, 365.
19 F. Neve, M. Ghedini and A. Crispini, *J. Organomet. Chem.*, 1994, **466**, 259.
20 L. Latos-Grazynski, J. Lisowski, M. M. Olmstead and A. L. Blach, *Inorg. Chem.*, 1989, **28**, 1183.
21 L. Latos-Grazynski, M. M. Olmstead and A. L. Blach, *Inorg. Chem.*, 1989, **28**, 4066.
22 G. van Stein, G. van Koten, F. Blank, L. C. Taylor, K. Vrieze, A. L. Spek, A. J. M. Duisenberg, A. M. M. Scheurs, B. Kojic-Prodic and C. Brevard, *Inorg. Chim. Acta*, 1985, **98**, 107.
23 E. C. Constable, R. P. G. Henney and D. A. Tocher, *J. Chem. Soc., Chem. Commun.*, 1986, 913.
24 E. C. Constable, S. J. Dunne, D. G. F. Rees and C. X. Schmitt, *Chem. Commun.*, 1996, 1196.
25 A. Varshney and G. M. Gray, *Inorg. Chim. Acta*, 1988, **148**, 215.
26 T. M. Räsänen, S. Jääskeläinen and T. A. Pakkanen, *J. Organomet. Chem.*, 1998, **553**, 453.
27 M. C. Barral, R. Jimenez-Aparicio, R. Kramolowsky and I. Wagner, *Polyhedron*, 1993, **12**, 903.
28 D. G. Dick and D. W. Stephan, *Can. J. Chem.*, 1986, **64**, 1870.
29 U. Bodensieck, H. Vahrenkamp, G. Rheinwald and H. Stoekli-Evans, *J. Organomet. Chem.*, 1995, **488**, 85.
30 A. J. Deeming, S. N. Jayasuriya, A. J. Arce and Y. De Sanctis, *Organometallics*, 1996, **15**, 786.
31 A. J. Deeming, S. N. Jayasuriya, A. J. Arce and Y. De Sanctis, *J. Chem. Soc., Dalton Trans.*, 1999, 1153.
32 J. D. King, M. Monari and E. Nordlander, *J. Organomet. Chem.*, 1999, **573**, 272.
33 A. R. Sanger, *Can. J. Chem.*, 1984, **62**, 2168.
34 M.-G. Choi and R. J. Angelici, *Organometallics*, 1992, **11**, 922.
35 S. Harris, *Polyhedron*, 1997, **16**, 3219.
36 B. Bak, D. Christensen, L. Hansen-Nygaard and J. Rastrup-Andersen, *J. Mol. Spectrosc.*, 1961, **6**, 61.
37 T. B. Rauchfuss, D. M. Roundhill and F. T. Patino, *Inorg. Chem.*, 1975, **14**, 652.
38 M. Draganjac, T. B. Rauchfuss and A. L. Rheingold, *Proc. Arkansas Acad. Sci.*, 1992, **46**, 36.
39 P. A. Chaloner, S. R. Gunatunga and P. B. Hitchcock, *J. Chem. Soc., Perkin Trans. 2*, 1997, **8**, 1597.
40 T. A. Stephenson and G. Wilkinson, *J. Inorg. Nucl. Chem.*, 1966, **28**, 945.
41 R. P. Schutte, S. J. Rettig, A. M. Joshi and B. R. James, *Inorg. Chem.*, 1997, **36**, 5809.

42 E. Lindner, A. Moeckel, H. A. Mayer and R. Fawzi, *Chem. Ber.*, 1992, **125**, 1363.
43 D. W. Krassowski, J. H. Nelson, K. R. Brower, D. Hauenstein and R. A. Jacobson, *Inorg. Chem.*, 1988, **27**, 4294.
44 M. S. Lupin and B. L. Shaw, *J. Chem. Soc. A*, 1968, 741.
45 C. F. J. Barnard, J. A. Daniels, J. Jeffery and R. J. Mawby, *J. Chem. Soc.*, *Dalton Trans.*, 1976, 953.
46 J. Jeffery and R. J. Mawby, *J. Organomet. Chem.*, 1972, **40**, C42.
47 E. Lindner, U. Schroeber, R. Fawzi, W. Hiller, U. Englert and P. Wegner, *Chem. Ber.*, 1987, **120**, 1621.
48 E. Lindner and A. Bader, *Coord. Chem. Rev.*, 1991, **108**, 27.
49 N. DiCesare, M. Belletete, C. Marrrano, M. Leclerc and G. Durocher, *J. Phys. Chem. A*, 1999, **103**, 795.
50 T. A. Skotheim, R. L. Elsenbaumer and J. R. Reynolds, *Handbook of Conducting Polymers*, Marcel Dekker, New York, 1998.
51 G. M. Sheldrick, Bruker AXS, Madison, WI, 1997.
52 Crystal Structure Analysis Package, Molecular Structure Corporation, The Woodlands, TX, 1985 and 1992.
53 C. K. Johnson, ORTEP, Report ORNL-5138, Oak Ridge National Laboratory, Oak Ridge, TN, 1976.
54 H. Storflor and J. Skramstad, *Acta Chem. Scand. B*, 1986, **40**, 178.
55 A. Carpita and R. Rossi, *Gazz. Chim. Ital.*, 1985, **115**, 575.